

## Supporting Information for

### Printed Microfluidic Sweat Sensing Platform for Cortisol and Glucose Detection

Aditi R. Naik,<sup>1,a</sup> Yiliang Zhou,<sup>1,a</sup> Anita A. Dey,<sup>1,b</sup> D. Leonardo González Arellano,<sup>a</sup> Uzodinma Okoroanyanwu,<sup>a</sup> Ethan B. Secor,<sup>c</sup> Mark C. Hersam,<sup>c,d</sup> Jeffrey Morse,<sup>a</sup> Jonathan P. Rothstein,<sup>b</sup> Kenneth R. Carter,<sup>a</sup> and James J. Watkins<sup>a,\*</sup>

<sup>a</sup> Department of Polymer Science and Engineering, University of Massachusetts, Amherst, Massachusetts 01003, United States

<sup>b</sup> Department of Mechanical and Industrial Engineering, University of Massachusetts, Amherst, Massachusetts 01003, United States

<sup>c</sup> Department of Materials Science and Engineering, Northwestern University, Evanston, Illinois 60208, United States

<sup>d</sup> Department of Chemistry, Northwestern University, Evanston, Illinois 60208, United States

\*Corresponding author: watkins@polysci.umass.edu

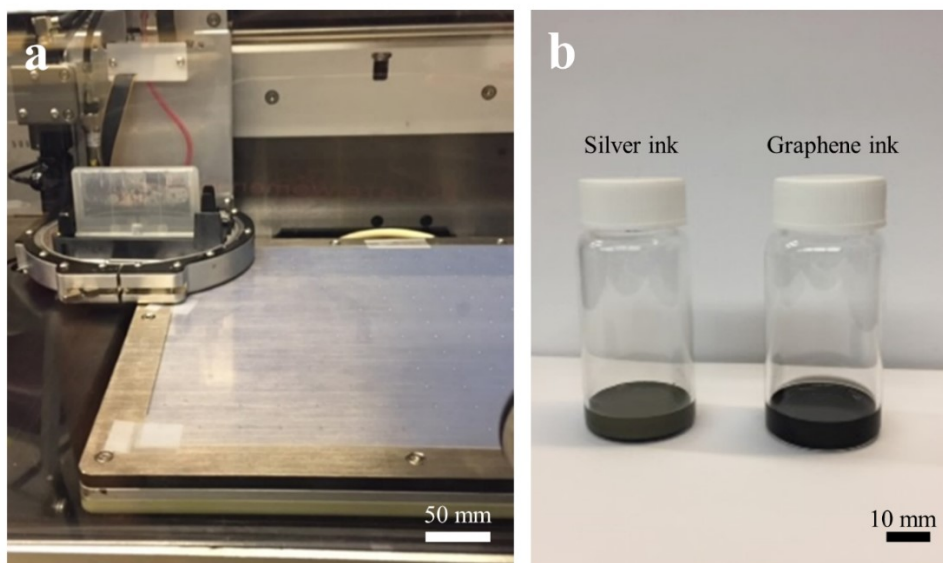


**Figure S1.** Inkjet printer and ink formulations. (a) Inside of Dimatix printer showing the disposable ink cartridge. (b) Images of the silver ink and graphene ink in scintillation vials.

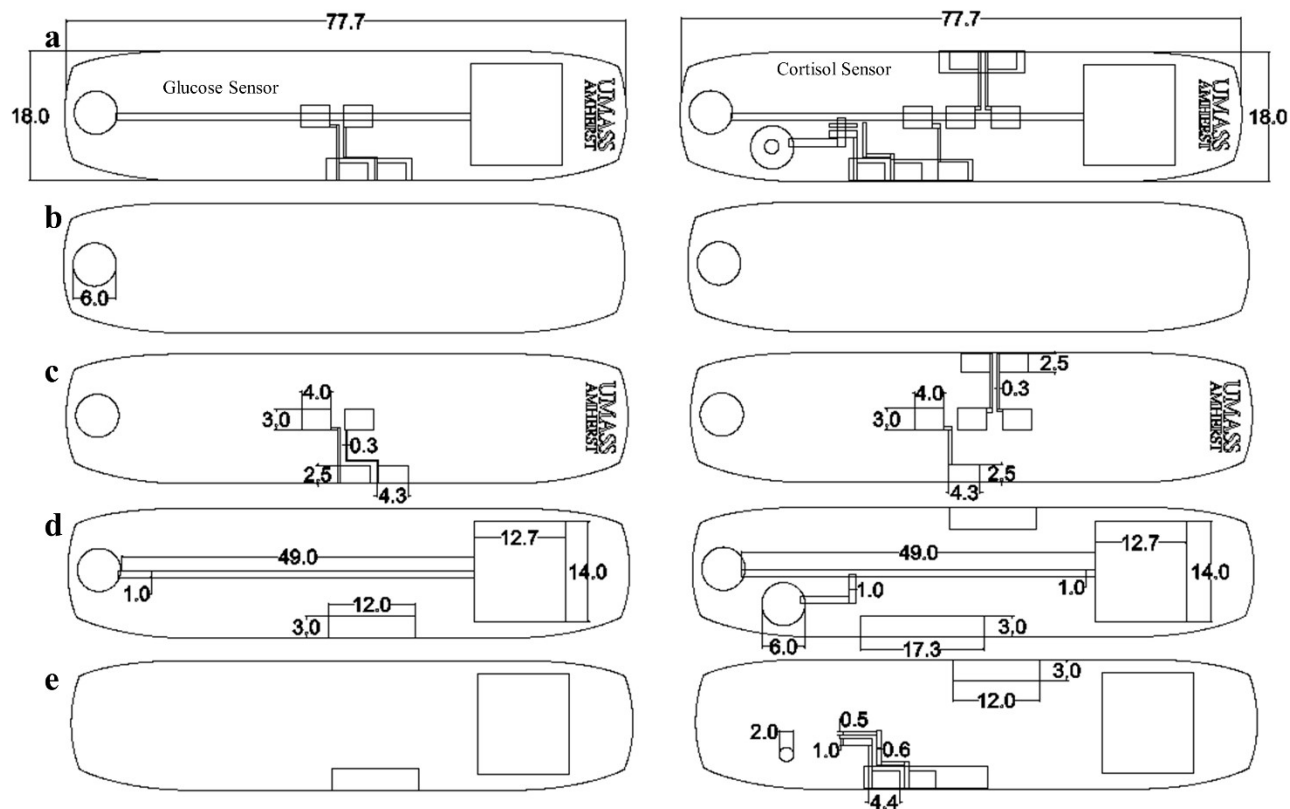


**Figure S2.** Dimensions of glucose (left) and cortisol (right) sensors. (a) Full sensor and microfluidic design, (b) Conformal skin adhesive used to adhere the device to the synthetic skin, (c) Inkjet-printed sensor electrodes and connectors on PI substrate, (d) Microchannels cut from pressure-sensitive adhesive to allow for fluid flow and adhere the PI and PET substrates, (e) PET top layer to seal microfluidic device with located for electrical connections to electrodes and replaceable absorbent pad.

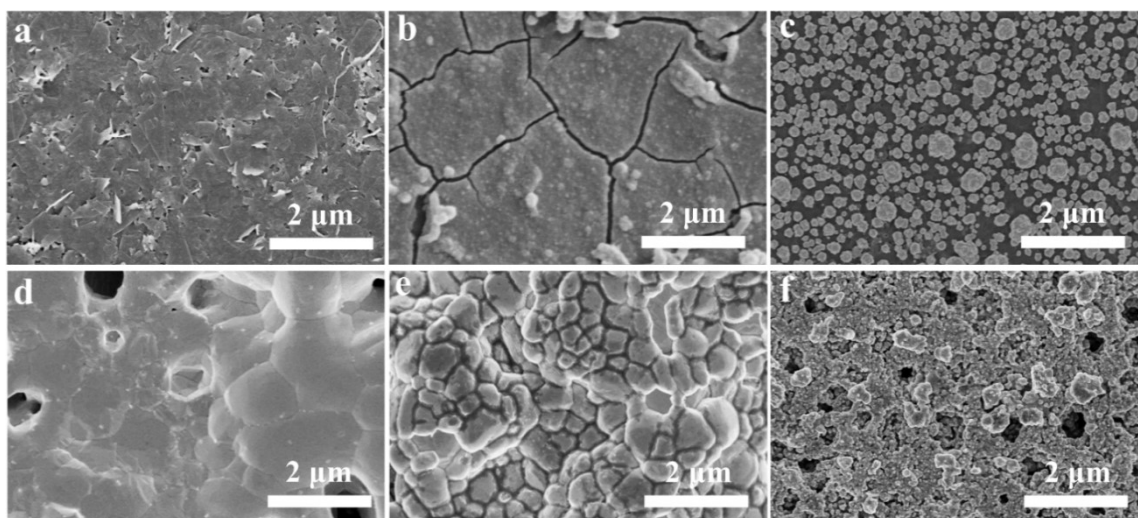


**Figure S3.** SEM images of printed electrodes. (a) Annealed printed graphene electrode on PI substrate. (b) Electrodeposited PB layer over graphene electrode. (c) Electrodeposited gold layer over graphene electrode. (d) Annealed printed silver ink on PI substrate. (e) Ag/AgCl electrode. (f) PFDT-modified silver ink on PET substrate. Samples were coated with 2 nm Pt for imaging.

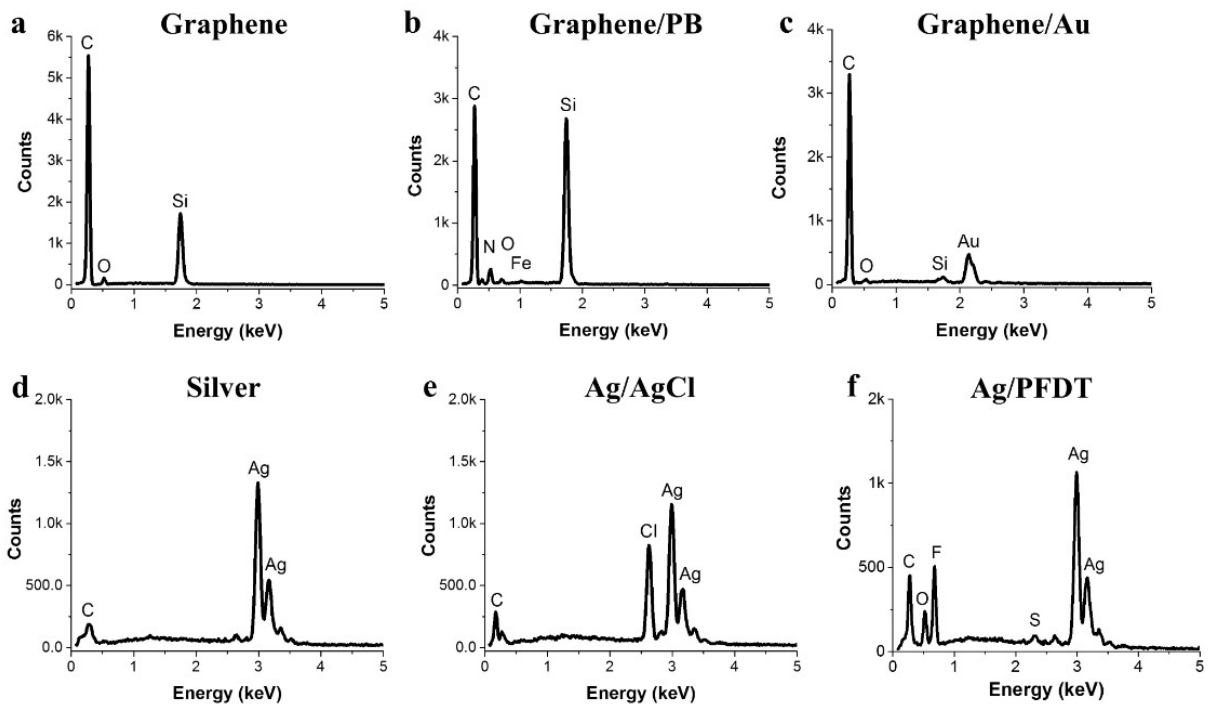


**Figure S4.** EDS spectra. (a) Printed annealed graphene electrode. (b) PB-modified graphene electrode. (c) Au-modified graphene electrode. (d) Printed annealed silver electrode. (e) AgCl-modified silver electrode. (f) PFDT-modified silver electrode.

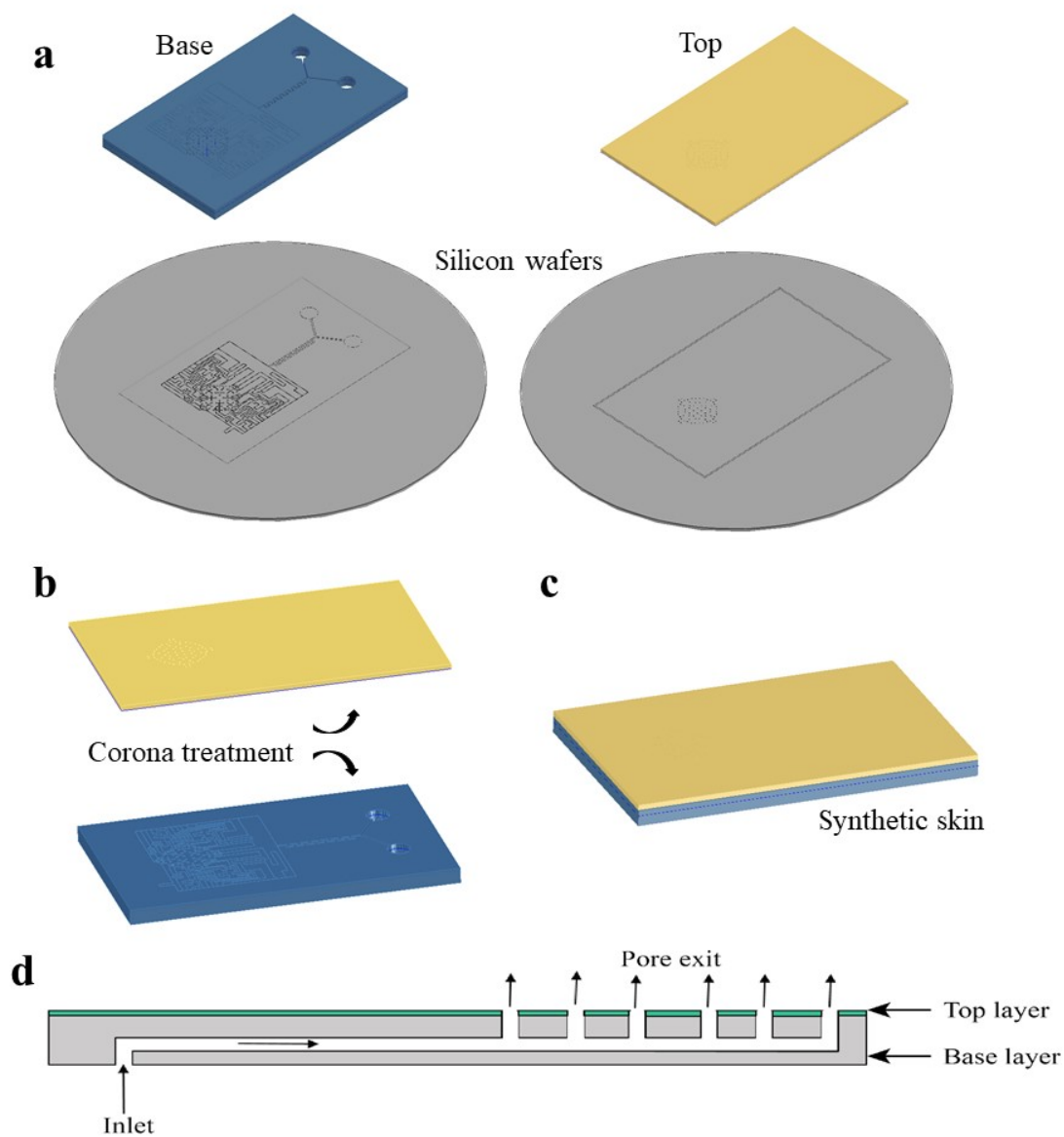


**Figure S5.** Schematic of synthetic skin assembly. (a) Polydimethylsiloxane (PDMS) base and top layers produced from silicon wafer masters using soft lithography. (b) Corona treatment of the inner surfaces of the layers. (c) Alignment and sealing of the base and top layers of the synthetic skin. (d) Simplified flow path of sweat through the assembled layers of the synthetic skin.

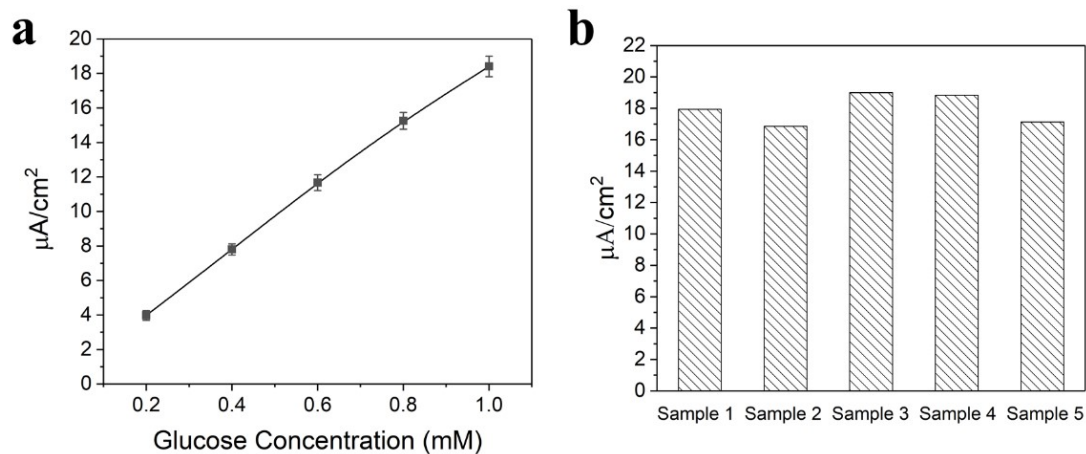


**Figure S6.** Glucose sensor characterization. (a) Calibration curve of GOx/PB-graphene electrode for detection of glucose. (b) The reproducibility of glucose biosensor with PB-graphene electrode in 0.1 mM glucose concentration.

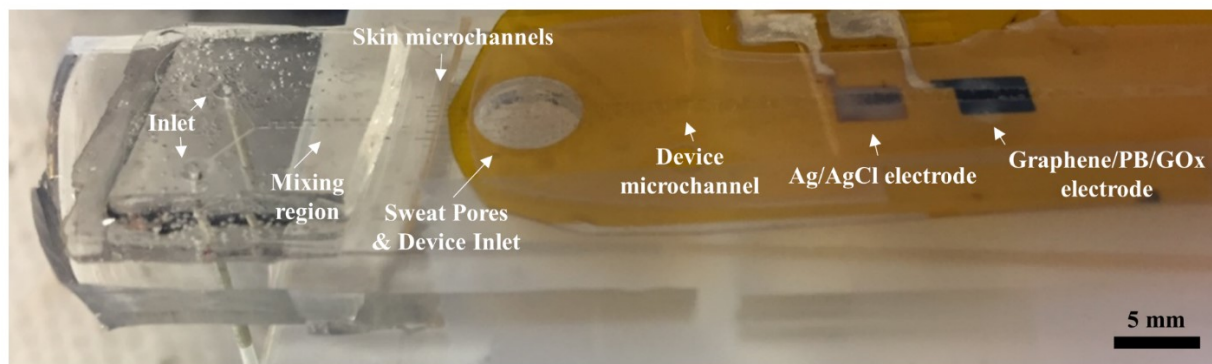


**Figure S7.** Glucose sensor and synthetic skin assembly. (a) Synthetic skin shown with two inlets, mixing channel and microchannels within the synthetic skin, and sweat pores in contact with device inlet with a microchannel leading to the sensor electrodes.

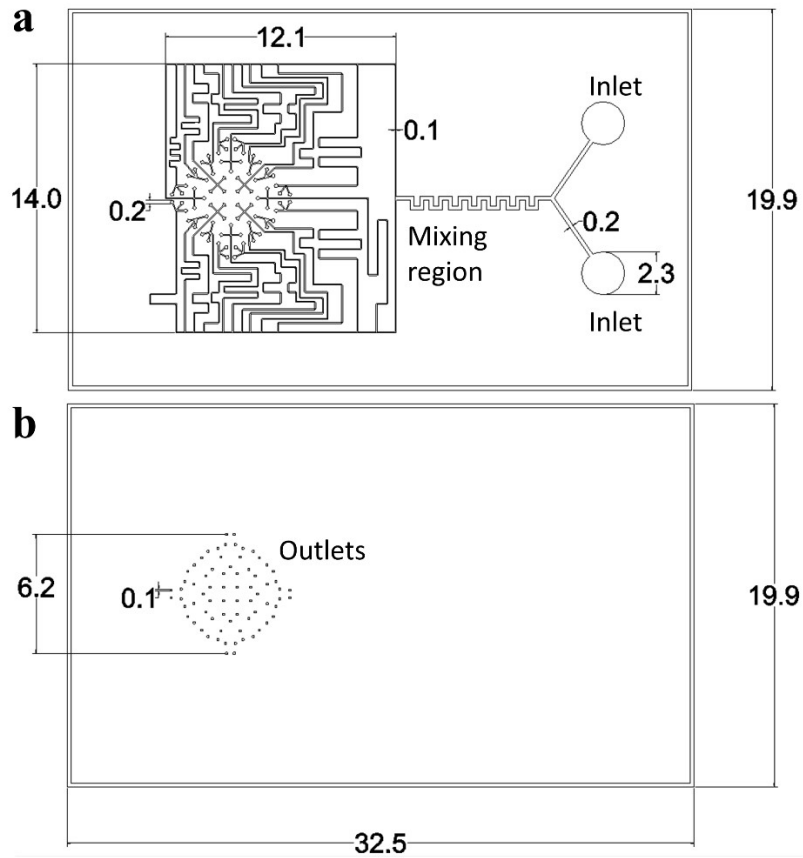


**Figure S8.** Mask dimensions for synthetic skin. (a) Bottom base channel layer of synthetic skin showing two inlets, mixing region, and skin microchannels leading to sweat pores. (b) Top porous layer with sweat pores. Units are in mm.

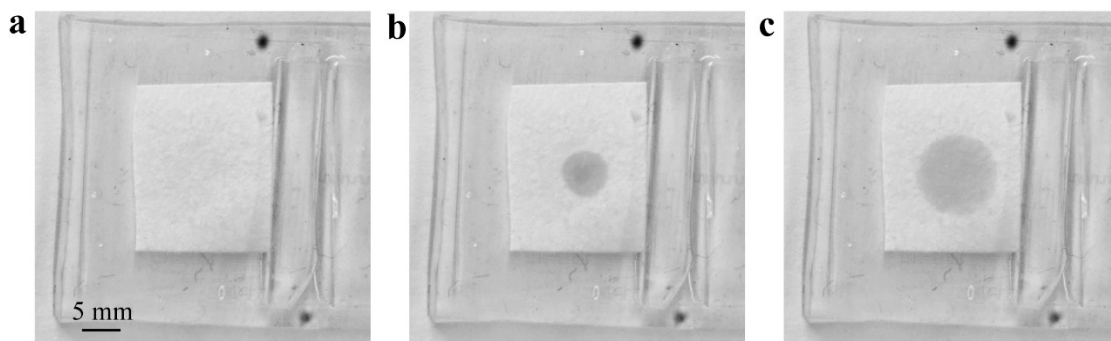


**Figure S9.** Skin sweat production. (a-c) Sequence of images captured at the start of sweat production over a time interval of 0.5 s at a flow rate of 1  $\mu\text{L}/\text{min}$ . Absorbent pad placed over skin pores to visualize sweat production.